Aromatic-Aromatic Interactions: Free Energy Profiles for the Benzene Dimer in Water, Chloroform, and Liquid Benzene

William L. Jorgensen*,† and Daniel L. Severance

Contribution from the Department of Chemistry, Purdue University, West Lafayette, Indiana 47907. *Received November 27, 1989*

Abstract: An all-atom model for benzene is reported and tested largely in Monte Carlo simulations of pure liquid benzene, benzene in dilute aqueous solution, and the benzene dimer in water and chloroform. Free energy profiles were obtained for the association of the benzene dimer in liquid benzene, water, and chloroform that characterize the energetics for this prototypical interaction between arenes in solution. In all cases a contact dimer with a ring center-ring center separation of ca. 5.5 Å is found to be energetically preferred. Face-to-face stacked structures are net repulsive. However, gas-phase optimizations indicate that shifted, stacked structures become increasingly favorable with increasing arene size. Comparisons are made with key experimental data, including the free energy of hydration of benzene and the association constant, K_a, for the benzene dimer in water. The agreement with the results from the new potential function provides a basis for confidence in the accompanying insights of relevance to molecular design.

Interactions between aromatic rings are emerging as significant elements that can influence the stereochemistry of organic reactions,[1] binding affinities in host-guest chemistry,[2] and protein stability.[3] Their relevance to the structure and chemistry of nucleic acids is also well appreciated.[4] In view of the latter knowledge, the focus is often on stacked arrangements of aromatic rings. However, there is evidence that the prototypical case, benzene, prefers to form a T-shaped dimer in the gas phase[5,6] and that this preference carries over to crystalline benzene[7] and somewhat to the juxtaposition of aromatic side chains in the interior of proteins.[3] The stacked versus T-shaped issue is an important one in the design of organic host molecules for aromatic substrates.[8] Though the stacked motif has been emphasized, the binding enhancements that have been obtained so far upon addition of an aromatic stacking interaction have typically been modest, ca. 0.5 kcal/mol.[2a,b] This leads one to wonder just how much can be expected energetically from aromatic-aromatic interactions and if stronger binding might be obtainable via T-shaped designs. In order to make direct connections to the experimental studies,[1-3] these questions need to be addressed in solution, which then raises the additional complication of the solvent dependence of the results.

In the present paper, theoretical methods are used to help elucidate these issues primarily through studies of the benzene dimer in solution. Specifically, new potential function parameters have been obtained for benzene and are supported by thermodynamic and structural results for the gas-phase dimer, pure liquid benzene, and benzene in dilute aqueous solution. Subsequent, extensive calculations provided free energy profiles (potentials of mean force) for the separation of the benzene dimer in chloroform and water. This leads to insights on the merits of stacked and T-shaped structures in these solvents. Additional information on the competition is obtained from optimizations of complexes of benzene with naphthalene and anthracene in the gas phase.

Computational Elements

Intermolecular Potential Functions. Though six-site models for benzene are computationally attractive and are adequate to reproduce some thermodynamic properties of liquid benzene,[9] previous studies have established the benefits of 12-site models for proper descriptions of the structures of the liquid and crystalline phases.[6,7,10] Under the circumstances and in order to maintain compatibility with the OPLS potential functions for organic and biomolecular systems,[11] it was decided to investigate all-atom models for benzene with the intermolecular interactions described in a Coulomb plus Lennard-Jones format. This is detailed in eq 1 where the interaction energy between molecules a and b is

$$\Delta E_{ab} = \sum_{i}^{\text{on a}} \sum_{j}^{\text{on b}} (q_i q_j e^2/r_{ij} + A_{ij}/r_{ij}^{12} - C_{ij}/r_{ij}^{6}) \qquad (1)$$

decomposed into the individual interactions between all pairs of sites on the two molecules. The Lennard-Jones parameters, σ_i and ϵ_i, are related to the A's and C's in eq 1 by $A_{ii} = 4\epsilon_i\sigma_i^{12}$ and $C_{ii} = 4\epsilon_i\sigma_i^{6}$, and the combining rules are $A_{ij} = (A_{ii}A_{jj})^{1/2}$ and $C_{ij} = (C_{ii}C_{jj})^{1/2}$.

For benzene, there are five adjustable parameters: σ and ϵ for carbon and hydrogen, and one charge variable since $q_C = -q_H$. The σ's and ϵ's were required to be consistent with other values,[11] so the principal fitting was just for the charge. Earlier work suggested that values of q_H between 0.1 and 0.2 should be considered.[6] The final decisions were based on fitting results of Monte Carlo simulations for liquid benzene primarily to the observed heat of vaporization and density,[12] as described below. We were also aware of the experimental C-C radial distribution function.[13] The resultant parameters are $\sigma_C = 3.55$ Å, $\epsilon_C = 0.07$ kcal/mol, $\sigma_H = 2.42$ Å, $\epsilon_H = 0.03$ kcal/mol, and $q_H = -q_C = 0.115$. For

† Address correspondence to this author at Department of Chemistry, Yale University, New Haven, Connecticut 06511.

(1) Evans, D. A.; Chapman, K. T.; Hung, D. T.; Kawaguchi, A. T. *Angew. Chem., Int. Ed. Engl.* **1987**, *26*, 1184 and numerous references therein.
(2) For representative papers, see: (a) Benzing, T.; Tjivikua, T.; Wolfe, J.; Rebek, J., Jr. *Science* **1988**, *242*, 266. (b) Muehldorf, A. V.; Van Engen, D.; Warner, J. C.; Hamilton, A. D. *J. Am. Chem. Soc.* **1988**, *110*, 6561. (c) Lehn, J.-M.; Schmidt, F.; Vigneron, J.-P. *Tetrahedron Lett.* **1988**, *29*, 5255. (d) Zimmerman, S. C.; Wu, W. *J. Am. Chem. Soc.* **1989**, *111*, 8054.
(3) (a) Burley, S. K.; Petsko, G. A. *Science* **1985**, *229*, 23. (b) Singh, J.; Thornton, J. M. *FEBS Lett.* **1985**, *191*, 1.
(4) Saenger, W. *Principles of Nucleic Acid Structure*; Springer-Verlag: New York, 1984.
(5) (a) Janda, K. C.; Hemminger, J. C.; Winn, J. S.; Novick, S. E.; Harris, S. J.; Klemperer, W. *J. Chem. Phys.* **1975**, *63*, 1419. (b) Steed, J. M.; Dixon, T. A.; Klemperer, W. *J. Chem. Phys.* **1979**, *70*, 4940.
(6) (a) Karlstrom, G.; Linse, P.; Wallqvist, A.; Jonsson, B. *J. Am. Chem. Soc.* **1983**, *105*, 3777. (b) Pettersson, I.; Liljefors, T. *J. Comput. Chem.* **1987**, *8*, 1139. (c) Allinger, N. L.; Lii, J.-H. *J. Comput. Chem.* **1987**, *8*, 1146. (d) Shi, X.; Bartell, L. S. *J. Phys. Chem.* **1988**, *92*, 5667.
(7) (a) Cox, E. G.; Cruickshank, D. W. J.; Smith, J. A. C. *Proc. R. Soc. London A* **1958**, *A247*, 1. (b) Williams, D. E. *Acta Crystallogr.* **1974**, *A30*, 71. (c) Hall, D.; Williams, D. E. *Acta Crystallogr.* **1975**, *A31*, 56. (d) Williams, D. E.; Starr, T. L. *Comput. Chem.* **1977**, *1*, 173.
(8) Rebek, J., Jr. *Science* **1987**, *235*, 1478.
(9) (a) Evans, D. J.; Watts, R. O. *Mol. Phys.* **1976**, *32*, 93. (b) Claessens, M.; Ferrario, M.; Ryckaert, J.-P. *Mol. Phys.* **1983**, *50*, 217. (c) Jorgensen, W. L.; Madura, J. D.; Swenson, C. J. *J. Am. Chem. Soc.* **1984**, *106*, 6638.
(10) Bartell, L. S.; Sharkey, L. R.; Shi, X. *J. Am. Chem. Soc.* **1988**, *110*, 7006.
(11) (a) Jorgensen, W. L.; Tirado-Rives, J. *J. Am. Chem. Soc.* **1988**, *110*, 1657. (b) Jorgensen, W. L.; Briggs, J. M. *J. Am. Chem. Soc.* **1989**, *111*, 4190. (c) Jorgensen, W. L.; Briggs, J. M.; Contreras, M. L. *J. Phys. Chem.* **1990**, *94*, 1683.
(12) *Selected Values of Physical and Thermodynamic Properties of Hydrocarbons and Related Compounds*; American Petroleum Institute Research Project 44; Carnegie Press: Pittsburgh, 1953.
(13) (a) Narten, A. H. *J. Chem. Phys.* **1977**, *67*, 2102. (b) Narten, A. H. *J. Chem. Phys.* **1968**, *48*, 1630.

0002-7863/90/1512-4768$02.50/0

the present study, parameters for water and chloroform were also required so the TIP4P[14] and OPLS[11c] models were adopted. In each case, the geometries of the monomers were based on experimental data including r(CC) = 1.40 Å and r(CH) = 1.08 Å for benzene.[15]

Fluid Simulations. Monte Carlo statistical mechanics simulations were carried out for liquid benzene, a single benzene molecule in water, and the benzene dimer in water and chloroform. All calculations were performed for systems with periodic boundary conditions in the isothermal–isobaric (NPT) ensemble at 25 °C and 1 atm. Standard procedures were used including Metropolis sampling and, for the solutions, preferential sampling.[11,16] In addition, the ranges for translations and rotations of the monomers were chosen to provide acceptance probabilities of ca. 40% for new configurations.

The simulations of pure benzene involved 128 monomers in a cubic cell ca. 27 Å on a side. Lengthy equilibration was performed in the course of optimizing the potential function parameters. Averaging for the final results occurred over an additional 3.5 × 10^6 configurations. The intermolecular interactions were spherically truncated at 13 Å based on the distances between ring centers, though a correction was made to the total energy for the Lennard–Jones interactions neglected beyong the cutoff.[9c]

A calculation was then performed to determine the free energy of hydration of benzene. This was done by making a single benzene molecule disappear in TIP4P water.[17] In fact, the 12-site model of benzene was converted to the previous 6-site model[9c] and then to a single Lennard–Jones atom approximating methane which had its free energy of hydration determined earlier.[17] 265 water molecules (ca. 20 × 20 × 20 Å) were used in this case with solvent–solvent and solute–solvent cutoffs of 8.5 and 9.5 Å, respectively, based on the O–O and O–ring center distances. The free energy changes were calculated n a series of simulations with statistical perturbation theory (SPT)[17,18] and double-wide sampling.[19] Five simulations were used for both the 12-site to 6-site and 6-site to methane mutations. Each simulation consisted of 0.5 × 10^6 to 1.5 × 10^6 configurations for equilibration, followed by 2.0 × 10^6 configuration of averaging.

The potential of mean force computations for the benzene dimer in TIP4P water and chloroform were performed by gradually perturbing the ring centers apart in steps of 0.2 Å (each center moved in or out by 0.1 Å) with SPT. We were concerned with possible cutoff artefacts on the asymptotic behavior, so large systems and cutoffs were used. For the solutions, 735 water molecules and 185 chloroform molecules were included in periodic cells ca. 25 × 25 × 38 and 26 × 26 × 39 Å, respectively. The line between the ring centers was initially oriented along the long axis in each simulation. In all cases, the cutoffs for the solvent–solvent and solute–solvent interactions were at 12 Å with quadratic feathering to zero over the last 0.5 Å. Each simulation involved preferential sampling, equilibration periods of 1.1 × 10^6 configurations, and averaging for 2 × 10^6 and 4 × 10^6 configurations for the chloroform and aqueous solutions. All SPT calculations were performed with the BOSS program on Gould 32/8750 and Silicon Graphics 4D computers in our laboratory.

Results and Discussion

Gas-Phase Structures and Interaction Energies. The structure of the benzene dimer in isolation has been addressed in many experimental and theoretical studies.[5-7,20,21] Various alternatives

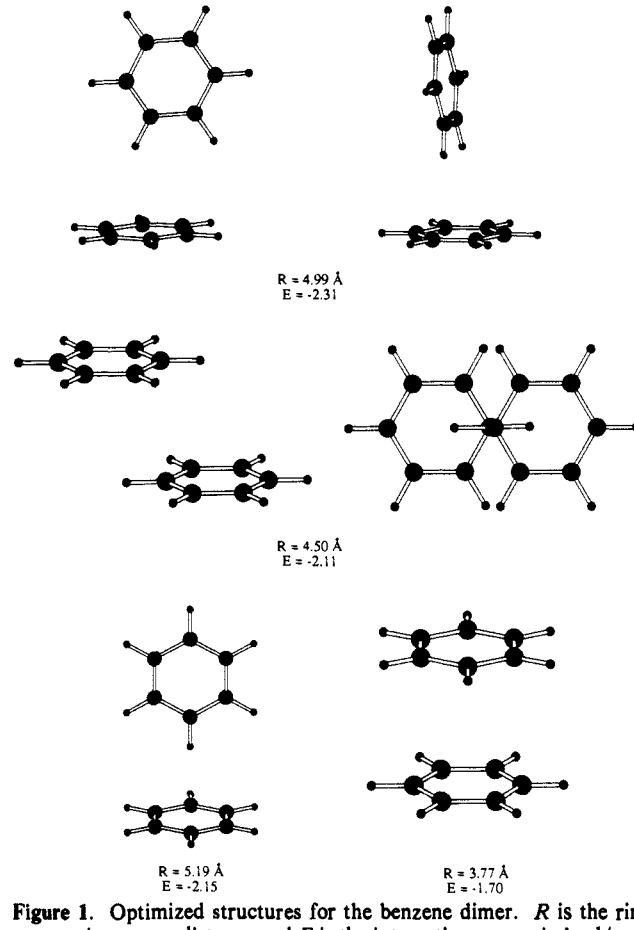

Figure 1. Optimized structures for the benzene dimer. R is the ring center–ring center distance and E is the interaction energy in kcal/mol.

were considered in optimizations with the present 12-site model. Some of the key results are summarized in Figure 1. A series of Monte Carlo optimizations indicates that the global minimum is the tilted T structure shown in two views at the top of the figure. The calculated interaction energy (−2.3 kcal/mol) agrees with the experimental value from a high-precision ionization measurement (−2.4 ± 0.4 kcal/mol)[22] and the best available ab initio results for T structures constrained to C_{2v} symmetry (−2.3 kcal/mol).[6a] Though molecular beam electric resonance experiments were interpreted to support a T structure,[5] alternative structures have been proposed on the basis of other spectroscopic measurements.[20,21] In particular, optical absorption spectra are consistent with a "parallel stacked and displaced" structure.[20] The present model yields an interaction energy of −2.1 kcal/mol for such a structure as shown by the two views in the middle of Figure 1. In this case the only constraint that was imposed was that the rings lie in parallel planes. The ring center–ring center separation is 4.5 Å versus 5.0 Å for the tilted T. A slightly lower energy (−2.15 kcal/mol) is obtained for the T structure constrained to have the ring planes perpendicular and one hydrogen nearest to the other ring (bottom left structure in Figure 1). There is no experimental support for a parallel stacked structure with coincident 6-fold symmetry axes. When constrained, the lowest energy structure of this type found here (bottom right structure in Figure 1) has an interaction energy of −1.70 kcal/mol and an interplane separation of 3.8 Å, a spacing similar to that between base pairs in nucleic acids.[4] It is interesting to note that the −1.70 kcal/mol energy consists of a repulsive Coulombic contribution of +1.37 kcal/mol, +1.96 kcal/mol from the $1/r^{12}$ terms, and −5.03 kcal/mol for the $1/r^6$ terms. On the other hand, the −2.31 kcal/mol for the tilted T structure is Coulombically attractive

(14) Jorgensen, W. L.; Chandrasekhar, J.; Madura, J. D.; Impey, R. W.; Klein, M. L. *J. Chem. Phys.* **1983**, *79*, 926.
(15) Bastiansen, O. *Acta Crystallogr.* **1957**, *10*, 861. Harmony, M. D.; Laurie, V. W.; Kuczkowski, R. L.; Schwendeman, R. H.; Ramsey, D. A. *J. Phys. Chem. Ref. Data* **1979**, *8*, 619.
(16) (a) Metropolis, N.; Rosenbluth, A. W.; Rosenbluth, M. N.; Teller, A. H.; Teller, E. *J. Chem. Phys.* **1953**, *21*, 1087. (b) Owicki, J. C. *ACS Symp. Ser.* **1978**, *No. 86*, 159.
(17) Jorgensen, W. L.; Blake, J. F.; Buckner, J. K. *Chem. Phys.* **1989**, *129*, 193.
(18) Zwanzig, R. W. *J. Chem. Phys.* **1954**, *22*, 1420.
(19) Jorgensen, W. L.; Ravimohan, C. *J. Chem. Phys.* **1985**, *83*, 3050.
(20) Law, K. S.; Schauer, M.; Bernstein, E. R. *J. Chem. Phys.* **1984**, *81*, 4871.
(21) Bornsen, K. O.; Selyle, H. L.; Schlag, E. W. *J. Chem. Phys.* **1986**, *85*, 1726.
(22) Grover, J. R.; Walters, E. A.; Hui, E. T. *J. Phys. Chem.* **1987**, *91*, 3233.

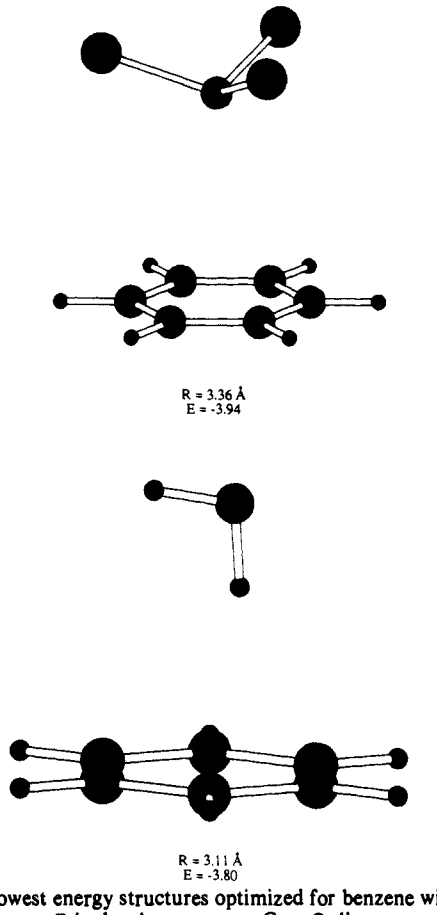

Figure 2. Lowest energy structures optimized for benzene with chloroform and water. R is the ring center to C or O distance.

Table I Thermodynamic Results for Liquid and Aqueous Benzene at 25 °C and 1 atm

property	calcd	exptl[a]
ΔH_{vap}, kcal/mol	8.05 ± 0.01	8.09
d, g cm^{-3}	0.873 ± 0.001	0.874
V, Å^3	148.6 ± 0.2	148.4
C_p, cal/mol·K	31.2 ± 1.0	32.5
ΔG_{hyd}, kcal/mol	−0.90 ± 0.39	−0.767[b]

[a] Reference 12. [b] Reference 23.

(−0.45 kcal/mol), has a similar $1/r^{12}$ contribution (+1.76 kcal/mol), and diminished $1/r^6$ attraction (−3.62 kcal/mol). In both cases, the $1/r^6$ van der Waals attraction dominates the net binding.

The global minima that were located by Monte Carlo searches for complexes of benzene with chloroform and water molecules are shown in Figure 2, using the present potential functions. Note that a 4-site model is used for chloroform so the hydrogen is implicit.[11c] The most favored position for both chloroform and water is roughly over the center of the ring, a Coulombically sensible choice. Also, the interaction energies are both ca. −3.9 kcal/mol, and the ring center to C and O distances are 3.4 and 3.1 Å. Ab initio results are available for benzene–water complexes;[6a] the global minimum appears to be similar to the one found here with an interaction energy of −3.15 kcal/mol and a ring center to O distance of roughly 3.2 Å.

Liquid Benzene. The principal thermodynamic results from the simulation of liquid benzene are included in Table I along with the experimental data. Since the molecular volume (or density) and heat of vaporization participated in the fitting, the accord with experiment is excellent. In addition, the liquid's heat capacity, computed in the usual way,[9c] is also reasonable with the new model. It should be noted that the statistical uncertainties for the computed quantities reported here are $\pm 1\sigma$ and were derived from separate averages over batches of typically 5×10^5 configurations in the Monte Carlo simulations.

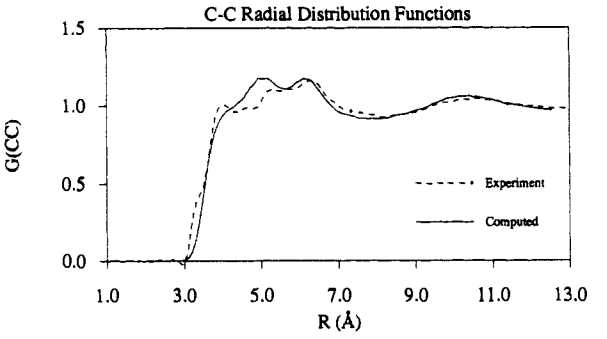

Figure 3. C–C radial distribution functions for liquid benzene at 25 °C.

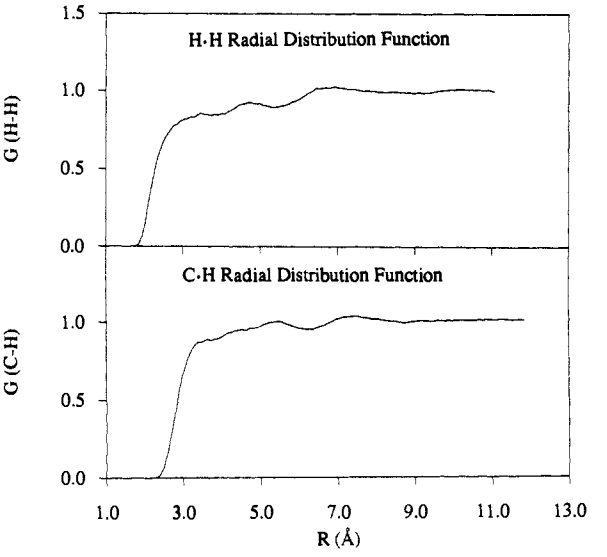

Figure 4. Computed C–H and H–H radial distribution functions for liquid benzene.

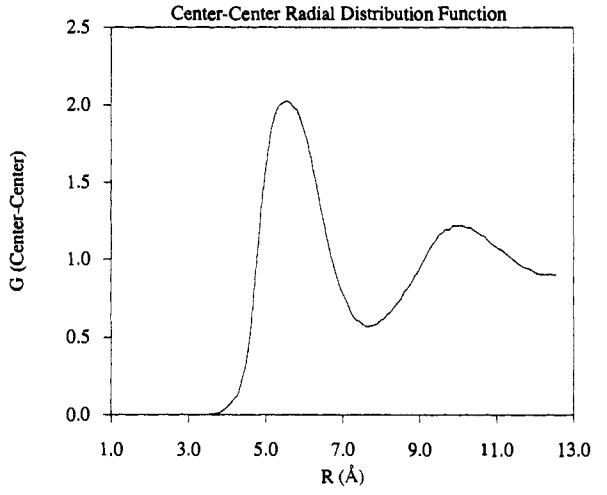

Figure 5. Computed ring center–ring center radial distribution function for liquid benzene.

The structure of the liquid is reflected in radial distribution functions, $g_{xy}(r)$, which give the probability of occurrence of atoms of type y at a distance r from atoms of type x, normalized for the bulk density of y atoms, $4\pi r^2(N_y/V)\,dr$. The three intermolecular atom–atom distributions are shown in Figures 3 and 4. Figure 3 also contains the C–C radial distribution function (rdf) determined by Narten from x-ray diffraction data for liquid benzene at 25 °C.[13a] The accord with the computed curve is pleasing, though not unexpected in view of the comparisons of results from electron diffraction experiments on benzene clusters and alternative 12-site potential functions.[10] In particular, the coincidence in Figure 3 for the peak positions and amplitudes is generally good. Furthermore, both theory and experiment find three features, two

peaks and a shoulder in the 3–7 Å region. By comparison, the C–H and H–H radial distribution functions (Figure 4) have little structure, as found previously.[10]

Information on the number of nearest neighbors is easier to extract from the ring center–ring center rdf shown in Figure 5. A well-resolved first peak with a maximum at 5.5 Å is now apparent and corresponds to the first shell of neighbors. Integration to the minimum at 7.5 Å yields 12 molecules in this shell. The same coordination number has been found experimentally in the solid[7] and liquid[13] and from prior theoretical studies including RISM calculations.[13a,24] The position of the first peak is consistent with contributions from T-shaped pairs, while the occurrence of parallel stacked dimers near their optimal separations of 3.8–4.5 Å (Figure 1) must be rare since the integral of the rdf to 4.5 Å only reveals 0.1 neighbor; integration even to 5.0 Å only accounts for 1 of the 12 neighbors in the first peak. It is notable that in the analysis of structures from the Brookhaven Protein Data Bank, Burley and Petsko obtained a distribution that resembles Figure 5.[3a] They plotted the normalized distribution of phenyl ring center–phenyl ring center separations and found a strong first maximum near 5.5 Å and a weak second maximum at about 9.5 Å. Singh and Thornton have also analyzed the geometries of Phe–Phe sidechain contacts in the Protein Data Bank.[3b] They found an essentially random distribution for the angle ϕ between the ring planes which favors perpendicular arrangements ($\phi = 90°$) owing to the intrinsic sin ϕ dependence. A similar analysis was performed here on the Monte Carlo results for liquid benzene. For ring center–ring center separations above 5 Å, sin ϕ behavior is basically followed. At shorter separations, the distribution for ϕ peaks at progressively lower angles, which reflects the steric constraints against larger ϕ's.

Dilute Aqueous Benzene. Strong motivation for going to a 12-site model of benzene with partial charges is provided by the realization that simpler models without electrostatic interactions are disposed to making the model benzene too hydrophobic. This was confirmed by the conversion of the Lennard-Jones 6-site model[9c] to methane in TIP4P water. It was previously established that the free energy of hydration of the model methane (corresponding to transfer of the solute from the ideal gas phase into infinitely dilute aqueous solution) is 2.27 ± 0.3 kcal/mol.[17] This value compares well with the experimental result of 2.005 kcal/mol; in all cases, standard states with molar concentration units are used in both phases.[17,23] The free energy of hydration of benzene is also known to be −0.767 kcal/mol.[23] Thus, experimentally the free energy of hydration of methane is 2.77 kcal/mol greater than that for benzene. However, the present SPT calculations with the 6-site model yielded a difference of only 1.06 ± 0.23 kcal/mol and a net free energy of hydration for the 6-site benzene of (2.27 ± 0.3) − (1.06 ± 0.23) = 1.2 ± 0.4 kcal/mol. The ca. 2 kcal/mol enhanced hydrophobicity for the model benzene would clearly distort solution-phase results in many contexts.

The problem can be resolved by the 12-site model owing to the added electrostatic interactions. SPT calculations were performed to convert the 12-site model to the 6-site model in TIP4P water, as described above. A free energy change of 2.11 ± 0.10 kcal/mol was obtained, which gives a net free energy of hydration of −0.9 ± 0.4 kcal/mol for the 12-site model (Table I). This result is in gratifying accord with the experimental value of −0.767 kcal/mol since it was obtained after the parametrization of the model was complete. However, the statistical uncertainty for the computed result, 0.4 kcal/mol, is significant. It is associated with the large perturbation involved in the complete removal of the benzene solute from water. Nevertheless, the cumulative results on the gas-phase dimer, pure liquid, and hydration of benzene reveal no obvious sources of concern for the present potential function's abilities to describe the energetics of benzene association in solution.

Earlier simulation studies of benzene in water should be noted.[25,26] Both groups used potential functions derived from ab initio calculations and extensively characterized the water structure around benzene from their Monte Carlo results. There is agreement that the first solvation shell contains about 23 water molecules including two water molecules on either side of the ring plane as in Figure 2. The earlier workers also attempted to calculate the energy of hydration of benzene from the ideal gas phase. However, in 1984 this was done by taking the difference between the average total energies for the complete system of benzene plus the N water molecules and for N water molecules without the solute. Since both numbers are large (ca. −2000 kcal/mol for $N = 200$) and fluctuating, the uncertainty in the computed energy of hydration was at least 30 kcal/mol.[25,26] The technical improvement with the SPT approach is striking.[19] The precision of the results is now certainly at the level where computed free energies of solvation can be used in the development and testing of potential functions.

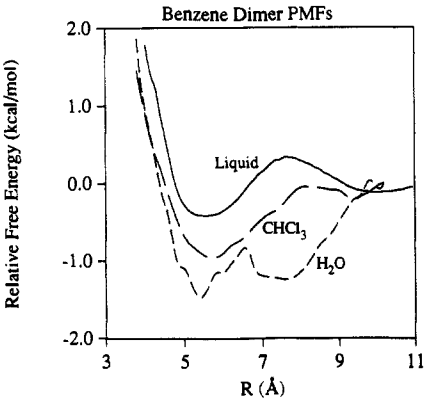

Figure 6. Computed potentials of mean force for the benzene dimer in liquid benzene, chloroform, and water. R is the ring center–ring center separation.

Benzene Association in Solution. The potential of mean force (pmf) for the separation of the benzene dimer was calculated by SPT in water and chloroform. The reaction coordinate for the perturbation was taken as the ring center–ring center distance. The corresponding pmf, $w(r)$, in liquid benzene is available from the center–center radial distribution function since $w(r) = -kT \ln g(r)$. The three potentials of mean force are shown in Figure 6.

A few technical points should be noted before the results are discussed further. First, 16 and 17 complete simulations were required for the calculations in chloroform and water to span the range of r from 3.4 or 3.8 Å to 10.2 Å. In these cases, the potentials of mean force have then been zeroed at 10.2 Å since only relative free energies are obtained from the SPT calculations. This probably introduces little error for the pmf in chloroform since it is flat within the statistical noise beyond 8 Å. The pmf in water is also flat beyond 9.6 Å; however, the curve has not obviously attained asymptotic behavior. It should be realized that the energy range in Figure 6 is narrow, so any shifting of the curves by rezeroing is unlikely to amount to more than a few tenths of a kcal/mol. Second, the results in all cases are supposed to be fully angularly averaged since the only constraint was on the center–center distance. Though the symmetry of benzene helps in this regard, the implied question is basically a matter of convergence. There is no doubt about the precision/convergence of the pmf for pure liquid benzene since the $g(r)$ was averaged over all pairs of molecules in the liquid, 127 pairs per configuration. The similarity of the results in chloroform to those in benzene is reasonable and along with the smoothness of these two pmf's is reassuring for the pmf in chloroform. Concern is more warranted for the pmf in water owing to the greater cohesiveness of the solvent, which hinders rotational diffusion of the solutes. Some sense of the convergence in this case is provided in Figure 7, which

(23) Ben-Naim, A.; Marcus, Y. *J. Chem. Phys.* **1984**, *81*, 2016.
(24) Lowden, L. J.; Chandler, D. *J. Chem. Phys.* **1974**, *61*, 5228.
(25) Linse, P.; Karlstrom, G.; Jonsson, B. *J. Am. Chem. Soc.* **1984**, *106*, 4096.
(26) Ravishanker, G.; Mehrotra, P. K.; Mezei, M.; Beveridge, D. L. *J. Am. Chem. Soc.* **1984**, *106*, 4102.

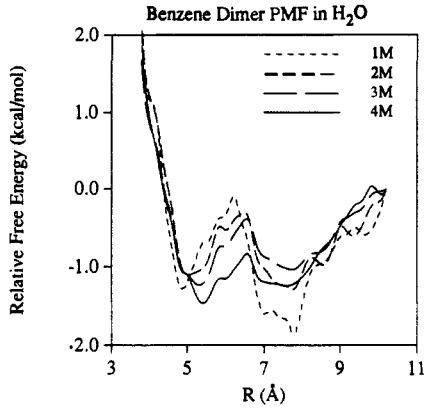

Figure 7. Evolution of the computed potential of mean force for the benzene dimer in water. Results are shown after averaging for 1–4-million configurations for each increment in R.

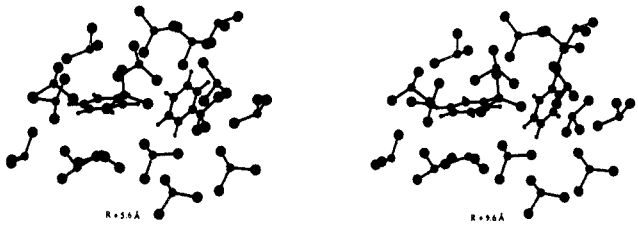

Figure 8. Stereoview of a random configuration for the benzene dimer in chloroform near the free energy minimum. Only chloroform molecules with an atom within 4.0 Å of a benzene atom are shown. A hydrogen is implicit on each chloroform molecule.

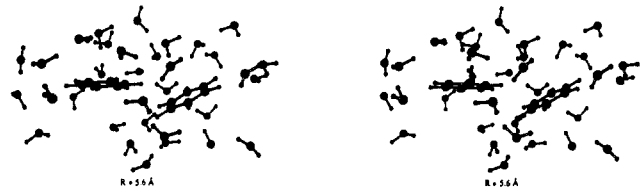

Figure 9. Random configuration for the benzene dimer in water in the vicinity of the contact minimum. Only water molecules with an atom within 3.5 Å of a benzene atom are shown.

displays the pmf in water after 1-, 2-, 3-, and 4-million configurations of averaging and the 1.1-million configurations of equilibration for each of the 16 simulations. The changes from 2- to 4-million configurations are modest particularly for the depths of the free energy wells centered near 5.5 and 7.5 Å, though there is a progressive diminution of the barrier near 6.5 Å. It is apparent that the pmf is changing slowly. This means that the results are reasonably well converged or that attainment of precise results would require great extension of the computations. Additional support for the former position is provided by the results below for the association constant, K_a, in water.

Figure 6 contains the key information on the energetic impact of aryl–aryl interactions in the prototypical case. In all three media, the optimal interaction occurs at a separation of about 5.5 Å corresponding to a contact dimer. Graphical analyses of configurations from the simulations near this separation reveal predominantly a range of distorted T-shaped pairs, including some roughly parallel stacked and displaced structures that can be regarded as part of the pathway between distorted T's. Two random examples, the last configurations in the simulations, are illustrated in Figures 8 and 9 for the chloroform and aqueous solutions. Only the nearest solvent molecules are shown. The example in Figure 8 is a distorted T-shaped pairing that is reminiscent of the lowest energy dimer in Figure 1, while the example in water (Figure 9) has more parallel, displaced character, though the rings do not overlap as in the middle structure in Figure 1. The benzene–benzene interaction energy is only −0.84 kcal/mol for the configuration in Figure 9 versus −1.78 kcal/mol for Figure 8. Though striking solute–solvent interactions are not plentiful

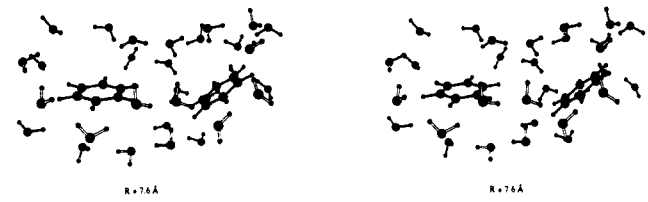

Figure 10. Random configuration for the benzene dimer in water in the vicinity of the solvent-separated minimum. Water molecules were selected as in Figure 9.

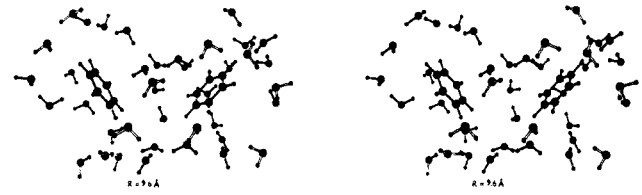

Figure 11. An alternative configuration for the benzene dimer in water as in Figure 10. A water cluster bridges between the ring faces in this case.

in the stereoviews, chloroform and water molecules are seen to take up some of the low-energy, face-solvating positions as in Figure 2.

In liquid benzene and chloroform, the only significant minimum is the contact one near 5.5 Å. For the aqueous solution, there is a second, presumably solvent-separated minimum near 7.5 Å. Random examples of two configurations near this separation are shown in Figures 10 and 11. The intersolute interaction energies in these examples are very modest, −0.32 and −0.09 kcal/mol, respectively. Though water is, in fact, not present between the edges of the rings in Figure 10, the arrangement in Figure 11 features a cluster of water molecules bridging between the two ring faces. It should be noted that pmf's have been computed previously for the methane dimer in water; in all cases contact and solvent-separated minima were found.[27-29] The picture in that case is of two clathrate cages sharing a common face between the solutes in the solvent-separated form.[28] In addition, in 1985 Ravishanker and Beveridge computed a pmf for separating the benzene dimer in water by importance sampling methods with the two rings constrained to be face-to-face with coincident 6-fold axes of symmetry.[30] Again, two minima were found; however, the asymptotic behavior and well-depths of ca. −5 kcal/mol do not seem reasonable (vide infra).

In Figure 6, the well-depths for the contact minimum are −0.4, −1.0, and −1.5 kcal/mol in liquid benzene, chloroform, and water. Thus, there appears to be a solvophobic enhancement of the binding on progression to more polar solvents. The optimal gas-phase interaction of −2.3 kcal/mol is considerably damped out by solvent competition and the entropic effects associated with the thermal, configurational averaging. So, in water or chloroform the most that can be expected for enhancement of binding by a phenyl–phenyl interaction is ca. 1 kcal/mol. Furthermore, the optimal enhancement is achieved for ring center–ring center separations near 5.5 Å. At separations near 4 Å where only face-to-face stacking is possible, the net interaction in solution is actually repulsive by ca. 1 kcal/mol, even though molecular mechanics calculations (Figure 1) indicate attraction of nearly 2 kcal/mol in the gas phase—caveat emptor. Such configurations are configurationally restricted, which translates to entropically unfavorable. The quantitative aspects of this discussion apply rigorously only to the present unconstrained aromatic–aromatic interaction; however, the qualitative results warrant consideration in molecular design.[2]

(27) Pangali, C.; Rao, M.; Berne, B. J. *J. Chem. Phys.* **1979**, *71*, 2975.
(28) Ravishanker, G.; Mezei, M.; Beveridge, D. L. *Faraday Symp. Chem. Soc.* **1982**, *17*, 79.
(29) Jorgensen, W. L.; Buckner, J. K.; Boudon, S.; Tirado-Rives, J. *J. Chem. Phys.* **1988**, *89*, 3742.
(30) Ravishanker, G.; Beveridge, D. L. *J. Am. Chem. Soc.* **1985**, *107*, 2565.

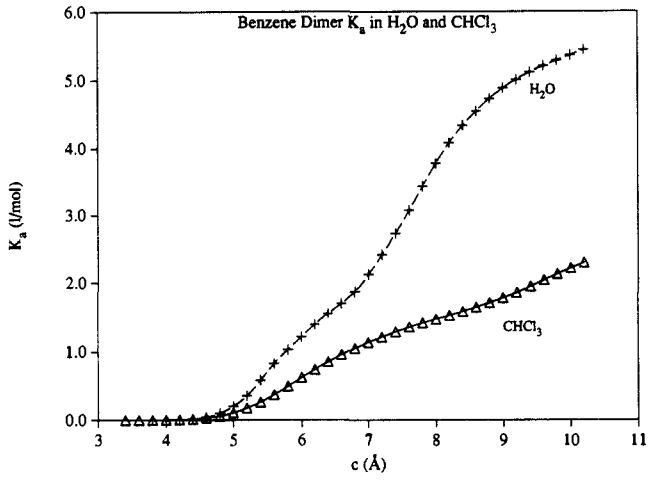

Figure 12. Computed association constants for the benzene dimer in water and chloroform as a function of the cutoff limit, *c*.

Important support for the accuracy of the pmf in liquid benzene is implicit in the good thermodynamic and structural results for the pure liquid that were discussed above. In the case of the dilute solutions, a key point of potential comparison between theory and experiment is for the association constant, K_a. Though experimental data are not available in chloroform, the K_a for the dimerization of benzene in water has been determined from Henry's law deviations. Two values have been reported, 0.85 M^{-1} at 35 °C and 0.5 M^{-1} in the range 15–40 °C.[31] It should be noted that these data are the only available experimental K_a's for hydrocarbons in water.[31]

On the theoretical side, K_a can be obtained from the potential of mean force via eq 2 where *c* is a cutoff that defines the geometrical limit to association.[32] The results from the pmf's in water

$$K_a = 2\pi \int_0^c r^2 \exp(-w(r)/k_BT)\, dr \qquad (2)$$

and chloroform are shown as a function of *c* in Figure 12. Though it is unclear what exact value of *c* should correspond to the Henry's law measurements, the computed K_a's are not extremely sensitive to the cutoff limit. Reasonable choices of *c*, e.g., 7–9 Å, which encompasses the region where $-w(r) > k_BT$,[32] give K_a's of 3 ± 1 in water and 1.5 ± 0.5 in chloroform. Thus, theory and experiment concur that the K_a in water is small, and it is predicted here that the K_a in chloroform is even smaller by a factor of about 2. In view of the exponential dependence of K_a on $w(r)$, substantial variation of the well-depth in water from the results in Figure 6 is unlikely. Thus, the well-depth of ca. −5 kcal/mol reported for the stacked dimer is unreasonable;[30] it possibly arose from incorrect zeroing of the pmf since the pmf was obtained only to a separation of 6.5 Å and the statistics from importance sampling tend to be poor at the ends of the sampling range.

An alternative approach for a comparison with the Henry's law data is to compute the osmotic second virial coefficient, $\bar{B}$, from McMillan–Mayer theory.[33] The relationship to the potential of mean force is given in eq 3 and involves no ambiguity in the

$$\bar{B} = -2\pi \int_0^\infty r^2[\exp(-w(r)/k_BT) - 1]\, dr \qquad (3)$$

integration limit. Evaluation of the expression from the computed pmf at 25 °C assuming $w(r) = 0$ beyond 10 Å yields $\bar{B} = -6.7 \times 10^3$ Å^3, while the experimental result at 35 °C is -1.2×10^3 Å^3.[31,33] Thus, the present results somewhat overestimate the association of benzene in water; scaling the pmf by a factor of 0.4 would bring the computed and experimental virial coefficients in line. For the pmf in chloroform, evaluation of eq 3 yields $\bar{B} = -1.4 \times 10^3$ Å^3 at 25 °C.

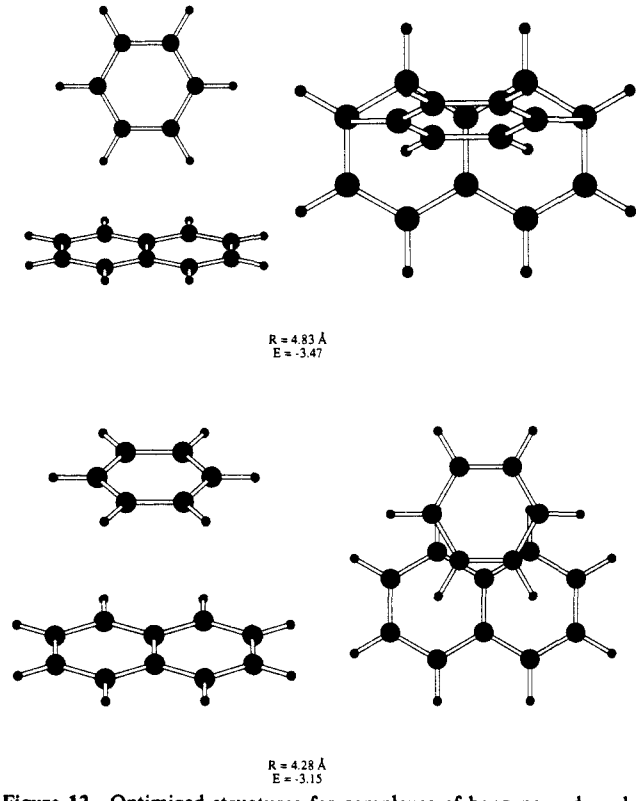

Figure 13. Optimized structures for complexes of benzene and naphthalene.

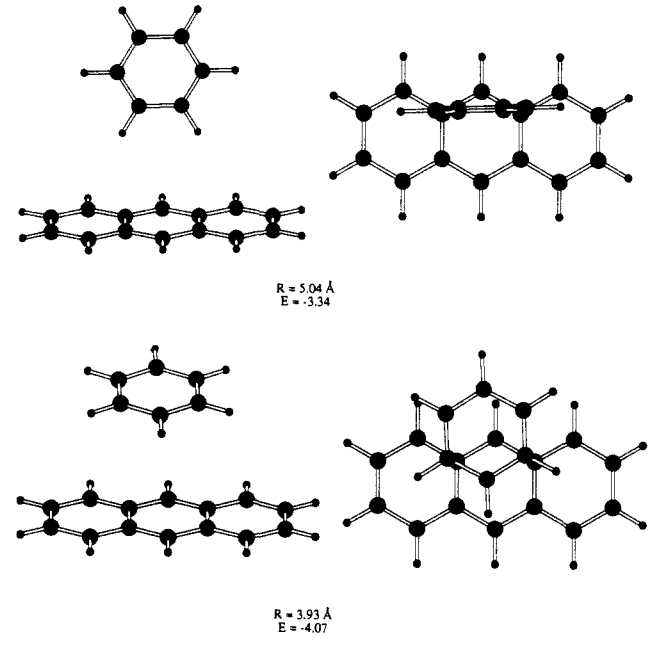

Figure 14. Optimized structures for complexes of benzene and anthracene.

Larger Aromatic Systems. To gain further insights on the competition between T-shaped and stacked structures, optimizations were also carried out for complexes of benzene with naphthalene and anthracene in the gas phase. For expediency, the parameters for the CH units were taken to be the same as for benzene, and the fusion carbons have the same σ and ϵ as for C in benzene, but no charge. Thus, the results are meant to be indicative but not definitive since the model for the larger aromatics has not been tested in fluid or crystal simulations.

The lowest energy T-shaped and stacked structures are shown in Figures 13 and 14. For the complexes with naphthalene, the

(31) (a) Tucker, E. E.; Christian, S. D. *J. Phys. Chem.* **1979**, *83*, 426. (b) Tucker, E. E.; Lane, E. H.; Christian, S. D. *J. Solution Chem.* **1981**, *10*, 1.
(32) (a) Justice, M.-C.; Justice, J.-C. *J. Solution Chem.* **1976**, *5*, 543. (b) Chandler, D.; Pratt, L. R. *J. Chem. Phys.* **1976**, *65*, 2925. (c) Shoup, D.; Szabo, A. *Biophys. J.* **1982**, *40*, 33. (d) Jorgensen, W. L. *J. Am. Chem. Soc.* **1989**, *111*, 3770.
(33) Rossky, P. J.; Friedman, H. L. *J. Phys. Chem.* **1980**, *84*, 587.

Table II. Energy Components (kcal/mol) for Arene Complexes

complex[a]	form[b]	Coulomb	$1/r^{12}$	$1/r^{6}$	total
BB	T	-0.45	1.76	-3.62	-2.32
	S	1.37	1.96	-5.03	-1.70
BN	T	-0.71	2.57	-5.34	-3.47
	S	0.35	2.74	-6.23	-3.15
BA	T	-0.57	2.08	-4.85	-3.34
	S	0.61	3.61	-8.29	-4.07

[a] B = benzene, N = naphthalene, A = anthracene. [b] T = T-shaped, S = stacked.

reported distances are between the center of the C9-C10 bond and the center of the benzene ring, while for anthracene the distance is between the center of the middle ring and the center of the benzene ring. A distorted T structure still has the lowest interaction energy (-3.5 kcal/mol) for the benzene-naphthalene pair. The lowest energy stacked structure in this case was located with the constraint that the rings lie in parallel planes. The interaction energy is -3.2 kcal/mol for the optimal form, which is displaced to have two benzene hydrogens roughly over the centers of the two naphthalene rings.

Upon increasing the system size further to anthracene, preference for a slightly tipped stacked structure finally emerges (Figure 14). The interaction energy of -4.1 kcal/mol is now 0.7 kcal/mol lower than that for the best T-shaped structure, which had to be located including a constraint that the ring planes be orthogonal. The stacked structure now has a benzene hydrogen near the center of each of the three rings in anthracene. However, the preference for the stacked structure is not electrostatic. As for the benzene dimers, the stacked structures are actually Coulombically repulsive, +0.35 and +0.61 kcal/mol for the complexes with naphthalene and anthracene, respectively. The binding for all of these systems is dominated by the van der Waals ($1/r^6$) attraction, as summarized in Table II. This term is favored by more densely packed arrangements, which leads to the preference for stacked structures as the size of the components increases. Some optimizations were also carried out for naphthalene and anthracene dimers; T-shaped and stacked structures are found to be nearly isoenergetic for the naphthalene dimers, while a strong preference for stacked anthracene dimers is obtained.

The key messages for molecular design from these results are that (1) stacked structures become more favorable with increasing size of the arenes and (2) the preferred geometry for stacked structures is offset with hydrogens roughly over ring centers. It may be noted that these notions are combined in the molecular tweezer of Zimmerman and Wu that shows a remarkable affinity for clamping adenine between two anthracene plates.[2d]

Conclusion

In the present paper, new potential function parameters have been reported for benzene that yield results in general accord with experimental data for the gas-phase dimer, pure liquid benzene, benzene in dilute aqueous solution, and the benzene dimer in water. It is recommended that this expanded model be incorporated into the description of aromatic groups in peptide residues.[11a] Furthermore, the present results have provided insights of value in molecular design, including estimates of the energetics of phenyl-phenyl interactions and observations on the disfavoring of face-to-face stacking of benzene in solution and on the enhanced favorability of stacked, shifted structures with increasing arene size. The value of condensed phase simulation work as a complement to experimental studies on molecular recognition and design has also been further demonstrated.[34]

Acknowledgment. Gratitude is expressed to the National Science Foundation and National Institutes of Health for support of this work. Dr. A. H. Narten kindly provided the experimental data displayed in Figure 3, and Professor Peter J. Rossky provided helpful insights.

(34) For recent reviews, see: (a) Beveridge, D. L.; DiCapua, F. M. *Annu. Rev. Biophys. Chem.* **1989**, *18*, 431. (b) Jorgensen, W. L. *Acc. Chem. Res.* **1989**, *22*, 184.

Investigation of the Electronic Excited States of $C_2H_3S^+$ and $C_2H_3O^+$ by Means of Collision Spectroscopy

P. Traldi,[†] M. Hamdan,*[,†] and Cristina Paradisi[‡]

Contribution from the C.N.R., Area di Ricerca di Padova, Corso Stati Uniti 4, 35100 Padova, Italy, and Centro Studio Meccanismi di Reazioni Organiche del C.N.R., Via Marzolo 1, 35131 Padova, Italy. *Received September 20, 1989*

Abstract: The electronic excited states of the gaseous ions $C_2H_3S^+$ and $C_2H_3O^+$ generated from a variety of precursor molecules by electron impact were investigated by means of translational energy spectroscopy (TES). The spectra of $C_2H_3S^+$ show three electronic transitions that can be assigned to $C_2H_3S^+$ ($\tilde{C} \leftarrow \tilde{X}^1A$), ($\tilde{D} \leftarrow \tilde{X}^1A$), and ($\tilde{A}^1A \rightarrow \tilde{X}^1A$). The observation of the latter transition and its measured energy is the first experimental evidence that this ion has a long-lived (ca. 2 μs) electronic excited state located at 2.7 eV above its ground state. The spectra of $C_2H_3O^+$ offer no evidence of long-lived excited states. However, two collisionally induced electronic transitions involving the $\tilde{X}^1A_1$ ground state and two upper electronic excited states are clearly evident. The relative intensities of both transitions are clearly dependent on the identity of the precursor molecule. This dependence is attributed to the formation of different structures of the incident $C_2H_3O^+$ ion. This deduction is in accord with earlier experimental data and high-level theoretical calculations.

The structure, reactivity, thermochemical properties, and fragmentation pathways of the gaseous ions $C_2H_3S^+$ and $C_2H_3O^+$ continue to attract considerable interest. In recent years a number of techniques have been used to investigate both ions, including collision spectroscopy,[1-3] ion cyclotron resonance,[4,5] photoionization,[4,6] and ab initio molecular orbital calculations.[7] Despite

[†] C.N.R., Area di Ricerca di Padova.
[‡] Centro Studio Meccanismi di Reazioni Organiche del C.N.R.

(1) Paradisi, C.; Scorrano, G.; Daolio, S.; Traldi, P. *Org. Mass Spectrom.* **1984**, *19*, 198.
(2) Cooks, R. G.; Mabud, Md. A.; Horning, S. R.; Yang, X.-Y.; Paradisi, C.; Traldi, P. *J. Am. Chem. Soc.* **1989**, *111*, 859.

0002-7863/90/1512-4774$02.50/0